

## Studying the effect of some additives to the borosilicate Glass on the neutron shielding properties

Saddam Jamel Abd-Noor \*, Ahmed Fadhil Mkhaimer 

Department of Physics, College of Education for Pure Science (Ibn Al-Haitham), University of Baghdad, Baghdad, Iraq.  
\*Corresponding Author.

Received 04/01/2024, Revised 22/03/2024, Accepted 24/03/2024, Published Online First 20/11/2024



© 2022 The Author(s). Published by College of Science for Women, University of Baghdad.

This is an open-access article distributed under the terms of the [Creative Commons Attribution 4.0 International License](https://creativecommons.org/licenses/by/4.0/), which permits unrestricted use, distribution, and reproduction in any medium, provided the original work is properly cited.

### Abstract

The development of radiation shielding material is important since radioactive sources are used in industry, medicine, and agriculture. As a result, more research and development has been put into looking into different glass systems based on their unique qualities for protecting against neutron radiation. This study focuses on investigating glass-based materials for neutron shielding purposes. This investigation delves into the neutron shielding properties of a mixture comprising Sodium Aluminum borosilicate glass ( $(\text{SiB}_2\text{Na}_2\text{Al}_2\text{O}_9)_X$ , with added reinforcement materials ( $(\text{SiC})_{100-X}$ ,  $(\text{TiB}_2)_{100-X}$ , and  $(\text{BiClO})_{100-X}$  ( $X=95, 80, 65,$  and  $50\%$ ), the mixtures are denoted as codes G1, G2 and G3 respectively. Results and calculations indicate that adding reinforcing materials to borosilicate glass in various quantities enhances rapid neutron removal ( $\Sigma_R$ ). An increased reinforcing material ratio reduces shielding half value layer (HVL) and mean free path (MFB) to neutron. Comparing theoretical results, adding titanium nitride ( $\text{TiB}_2$ ) as reinforcement to borosilicate glass yields the maximum neutron attenuation and the least HVL at  $X=50$ . Thus, the G2 shield is the best for neutron radiation protection.

**Keywords:** Fast neutron, Half-value layer, mean free path, Removal cross-section, Shielding material.

### Introduction

Nuclear technology is used in almost every area of life, including health, manufacturing, gardening, and power generation, for more than sixteen percent of the world's needs<sup>1-3</sup>. It has the huge potential to lead to innovations that help everyone<sup>4-6</sup>. The neutrons pose a material or radiation threat due to their strength because they are neutrally charged particles, and they can travel through matter over long distances without scattering or being absorbed<sup>7-9</sup>. Because these radiations have dangerous biological effects that can have a big impact on people's health, it is important to keep workers and regular people near these nuclear sites safe from dangerous radiation leaks. It is important to have enough

radiation protection in all of these situations. Because of this, Neutron shielding is considered one of the most important challenges in protecting the environment and public health from exposure to neutron radiation<sup>10-12</sup>.

An effective removal cross-section ( $\Sigma_R$ ) can be used to describe the sample's effect<sup>13,14</sup>. It is the same as an absorption cross-section. The concentration of material with low atomic numbers is crucial for decelerating the neutrons. If there is enough moderating material in the mixture, this process will determine how many neutrons are weakened. One essential consideration for neutron-shielding material involves using fillers with a higher

macroscopic cross section for neutron absorption<sup>15-17</sup>. Extensive research has been dedicated to monitoring and controlling neutron radiation due to its vital role in various applications such as nuclear reactors and radiation therapy<sup>18,19</sup>. Furthermore, appropriate radiation-transparent shielding materials are required in radiotherapy<sup>20</sup>. Glass compositions have been formulated to exhibit exceptional transparency and strong radiation absorption characteristics<sup>21-23</sup>. These borosilicate glass characteristics make them ideal for incorporation into certain protective materials. For this purpose, literature has published many works; for example, according to Lee et al.<sup>24</sup>, borosilicate glass was used as a mineral additive and fine aggregate to produce neutron shielding mortar. The use of borosilicate glass powder and aggregates together increased the compressive strength of the mortar mixture and could shield 86% additional thermal neutrons. It also controlled the expansion caused by the alkali-silica reaction (ASR) between the alkali in cement and the reactive silica in borosilicate glass aggregate. This suggests the possibility of using borosilicate glass for neutron shielding purposes Singh et al.<sup>25</sup> The study evaluated the gamma and neutron shielding properties of bismuth borosilicate glasses, specifically focusing on glasses with 20 mol% Bi<sub>2</sub>O<sub>3</sub>, which were found to be superior in shielding effectiveness. The research compared the buildup factors of the glasses with those of steel-magnetite concrete and lead and concluded that the glasses containing Bi<sub>2</sub>O<sub>3</sub> are promising materials for shielding applications. Salama et al.<sup>26</sup>. The study investigates the gamma radiation and neutron shielding properties of lithium sodium borosilicate glasses with varying concentrations of lead oxide

(PbO) through experimental analysis and theoretical calculations. The results confirm that glasses with lead concentrations of 5-25 mol% have suitable and comparable gamma attenuation coefficients, making them efficient, transparent materials for gamma-ray and neutron shielding. Rammah et al.<sup>27</sup> investigated the impact of lead and bismuth oxide insertion on a novel glass system of P (5,10, 15, 20, 25) mol% by calculating various parameters such as mass attenuation coefficient, linear attenuation coefficient, half and tenth value layer, mean free path, effective atomic number, exposure and energy absorption buildup factors, and fast neutron removal cross sections for the fabricated glasses. The results show that the prepared glasses are effective shielding materials for reducing fast neutrons and gamma rays. Yilmaz et al.<sup>28</sup> discussed the importance of radiation shielding in the nuclear industry and explored boron as a potential material for shielding. Boron, when combined with other materials, can provide strong shielding properties due to its large cross-section, making it suitable for various situations. Neutron shielding properties are considered one of the most important challenges in protecting the environment and public health from exposure to neutron radiation<sup>29-31</sup>. In this paper, we will study the potential effects of adding certain reinforcement materials (SiC), (TiB<sub>2</sub>) and (BiClO) to borosilicate glass, with a particular focus on its shielding properties against neutrons. In addition to their performance in preventing neutron radiation leakage, this research aims to use new reinforcement materials capable of absorbing neutrons, improving the efficiency of neutron shielding, and enhancing public safety.

## Materials and Methods

For study of the properties of neutron shielding material, mixture materials were used consisting of matrix material borosilicate glass (SiB<sub>2</sub>Na<sub>2</sub>Al<sub>2</sub>O<sub>9</sub>)<sub>x</sub> with the symbol (G) and reinforced with three compounds with different concentrations: silicon carbide (SiC)<sub>100-x</sub>, titanium nitride (TiB<sub>2</sub>)<sub>100-x</sub>, and bismuth oxychloride (BiClO)<sub>100-x</sub>, (X=95,80,65,50 % wt) which is named as follows G1, G2 and G3, The XCOM program

<https://physics.nist.gov/PhysRefData/Xcom/html/xcom1.html> was used to calculate the weight percentages of the elements present in the mixed materials at different concentrations<sup>32</sup>. Then, the following parameters were calculated:

### Removal cross sections of fast neutrons ( $\Sigma_R$ )

The absorption reaction is responsible for removing the cross-section of fast neutrons<sup>33</sup>. Choosing materials where interactions are less likely helps prevent effects caused by secondary radiation released after neutron interactions<sup>34</sup>. The neutron attenuation of a material can be determined by employing an exponential equation that considers the shield material's thickness and the neutron removal cross-section  $\Sigma_R$  ( $\text{cm}^{-1}$ )<sup>35</sup>.

$$I_x = I_o e^{-\Sigma_R x} \dots\dots\dots 1$$

Let us denote  $I_o$ : the incident beam intensity.

$I_x$ : the intensity after entering a material of thickness  $X$ .

$\Sigma_R$ : the neutron removal cross-section.

The total macroscopic cross-section of fast neutrons is the quantity that describes the probability of a neutron reaction occurring along the path it travels through the material. It is symbolized by the symbol ( $\Sigma_R$ ) and is measured in units ( $\text{cm}^{-1}$ ). In the case of compounds and mixtures, the total macroscopic cross-section of the fast neutron ( $\Sigma_R$ ) is the sum of the whole macroscopic mass cross-section of the attenuation for each element in the mixture ( $\Sigma/\rho$ )<sub>i</sub> multiplied by the molecular density of each component in the substance ( $\rho_i$ )<sup>36</sup>.

$$\Sigma_R = \sum_i \rho_i (\Sigma/\rho)_i \dots\dots\dots 2$$

To calculate each element's macroscopic mass cross-section for each, element  $\Sigma/\rho$  ( $\text{cm}^2/\text{g}$ ), the following empirical equation was used<sup>37</sup>:

$$\Sigma/\rho (\text{cm}^2/\text{g}) = 0.206 A^{-1/3} Z^{0.294} \dots\dots\dots 3$$

### Results and Discussion

#### The density of the composite materials( $\rho$ ):

The density values of the mixture were calculated using mathematical Eqs 6-9 by adding reinforcement materials to borosilicate glass at different concentrations, ranging from (0,5,20,35 and 50) %. Borosilicate has a lower density than the other

$Z$  and  $A$  represent the element's atomic number and weight, respectively.

#### The half-value layer for the neutrons (HVL)

It is the material's thickness that is necessary to attenuate the incident neutron flux to precisely fifty percent of its initial intensity; we also used the following equation to determine the (HVL)<sup>38</sup>:

$$\text{HVL (cm)} = 0.693/\Sigma_{\text{total}} \dots\dots\dots 4$$

#### The mean free path of the neutrons (MFP)

It is defined as the average distance traveled by the neutron without interaction inside the shielding material and is given by the following relationship<sup>39</sup>:

$$\text{MFP (cm)} = 1/\Sigma_{\text{total}} \dots\dots\dots 5$$

#### The density of the composite materials( $\rho$ ).

The density of mixture( $\rho$ ) samples used in this study was calculated from the following equations<sup>40,41</sup>:

$$W_c = W_f + W_m \dots\dots\dots 6$$

$$\psi = \frac{W_f}{W_c} \times 100\% \dots\dots\dots 7$$

$$V_f = \frac{1}{1 + [(1-\psi) \frac{\rho_f}{\rho_m}]} \dots\dots\dots 8$$

$$\rho = \rho_f V_f + (1 - V_f) \rho_m \dots\dots\dots 9$$

Where  $\psi$  = fraction weighted for reinforcement materials,  $V_f$  is the volume fraction,  $\rho_f$ ,  $\rho_m$  the reinforcement and matrix material density,  $W_f$  &  $W_m$  are the weight of reinforcement and matrix material, respectively, and  $W_c$ : the weight of the mixture material.

reinforcing materials shown in Table 1. The density increase depends on the type of additional reinforcement materials used and concentration<sup>42</sup>. The densities of the G1 and G2 contents increased a little. Nevertheless, the densities of the G3 content

significantly increase due to the high density of the reinforcement material (BiClO).

**Table 1. Density values for different mixtures**

Chemical formula	Density of composite	Name of group	V <sub>f</sub> (5%)	Density of mixture	V <sub>f</sub> (20%)	Density of mixture	V <sub>f</sub> (35%)	Density of mixture	V <sub>f</sub> (50%)	Density of mixture
SiB <sub>2</sub> Na <sub>2</sub> Al <sub>2</sub> O <sub>9</sub> (G)	2.23	G	-	-	-	-	-	-	-	-
SiC (1)	3.21	G1	0.03527	2.26457	0.14798	2.37501	0.27224	2.49679	0.40993	2.63173
TiB <sub>2</sub> (2)	4.52	G2	0.02531	2.28796	0.10980	2.48144	0.20990	2.71066	0.33037	2.98655
BiClO (3)	7.78	G3	0.01486	2.31248	0.06687	2.60111	0.13370	2.97206	0.22278	3.46641

Table 2. lists the elements that make up each constituent in increasing order based on their atomic weight, atomic number, and mass removal cross-section. Building a correct database of different elements' fast neutron removal cross-sections is essential to solving the neutron shielding problem.

**Table 2. Shows the partial removal cross-section of the elements included in the shield composition**

Element	A	Z	$\Sigma/\rho(\text{cm}^2/\text{g})$
B	10.811	5	0.058042764
C	12.0107	6	0.053117135
O	15.9994	8	0.044359931
Na	22.98977	11	0.035797516
Al	26.9815386	13	0.032310646
Si	28.0855	14	0.031194512
Cl	35.453	17	0.02726241
Ti	47.867	22	0.022865615
Bi	208.98	83	0.009468693

### Removal cross sections of fast neutrons:

The effective neutron removal cross-section  $\Sigma_R$  ( $\text{cm}^{-1}$ ) is a critical parameter in neutron shielding studies<sup>43</sup>. Higher values of this parameter mean better shielding ability<sup>10</sup>. The cross-section of a shield is influenced by the composition of its elements, particularly the type and density. When determining the total cross-section for neutron removal, the presence of light elements is crucial. Among these elements, boron stands out with a high-value removal cross-section. Increasing the proportion of boron in the shield will consequently increase the removal cross-section for fast neutrons ( $\Sigma_R$ )<sup>44,45</sup>. Tables 3-6 demonstrate that the mixture

G2[ (borosilicate) + (TiB<sub>2</sub>)] has a significantly higher concentration of boron in its chemical composition compared to the other mixtures; for this reason, this specific mixture has the largest total cross-sectional area, which is consistent with what H.O. Tekin and others found in previous studies<sup>28,46</sup>. On the other hand, the mixture G3[(borosilicate) + (BiClO)], the neutron attenuation values may be lower for bismuth oxychloride added to borosilicate glass due to the different neutron properties of the materials used. Neutrons can react differently with bismuth oxychloride than titanium nitride, resulting in less attenuation. The effect of these properties depends on the structure of the material and possible nuclear interactions. And bismuth concentration can influence the outcomes. This is consistent with what Singh et al.<sup>25</sup> in previous studies<sup>47</sup>. Consequently, the mixture (G2) is more effective in attenuating fast neutrons than the other mixtures. We notice ( $\Sigma_R$ ) (G2 > G1 > G3) as illustrated in Fig.1. The figure below shows the change in the values of the effective cross-section for the removal of fast neutrons with a change in the type of reinforcing material added by 50 percent.

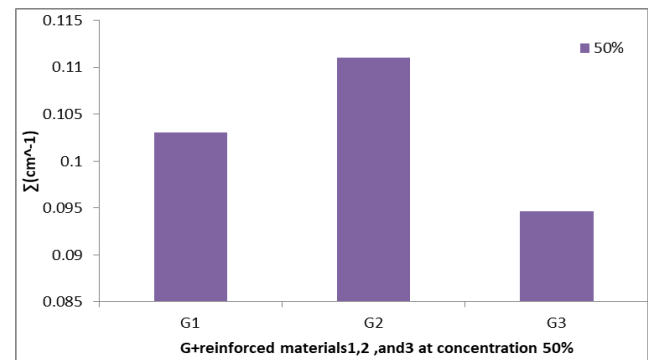


**Figure 1. Removal cross-section as a function of reinforced materials at a concentration of 50%**

Fig 2 Shows the relation between fast neutron removal cross-section and reinforcing material concentration. The figure shows that reinforcement material concentration directly affects the removal of cross-section values. With increasing concentration, the weighted fraction of the elements will also increase. Integrating reinforcement materials in different weight ratios improves neutron absorption and reduces their effects on the surrounding environment.<sup>48,49</sup>

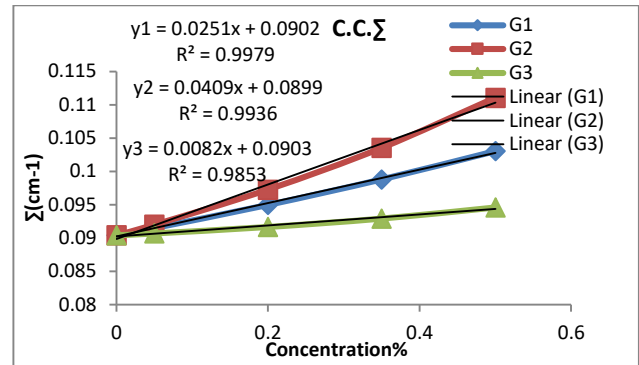


**Figure 2. Removal cross-sections as a function of concentration (%) and correlation coefficient**

**Table 3. Effective removal cross-section for group G**

Group	Concentration	Element	Composite Density(g/cm <sup>3</sup> )	Σ/ρ(cm <sup>2</sup> /g)	Fraction by Weight	Partial Density(g/cm <sup>3</sup> )	Σ(cm <sup>-1</sup> )	TotalΣ(cm <sup>-1</sup> )
G	0	Si	2.23	0.031194512	0.095645	0.21328835	0.00665343	0.09043367
		B		0.058042764	0.073633	0.16420159	0.00953071	
		Na		0.035797516	0.156582	0.34917786	0.0124997	
		AL		0.032310646	0.18377	0.4098071	0.01324113	
		O		0.044359931	0.49037	1.0935251	0.0485087	

**Table 4. Effective removal cross-section for group G+ SiC**

Group	Concentration	Element	Composite Density(g/cm <sup>3</sup> )	Σ/ρ(cm <sup>2</sup> /g)	Fraction by Weight	Partial Density(g/cm <sup>3</sup> )	Σ(cm <sup>-1</sup> )	TotalΣ(cm <sup>-1</sup> )
G1	0.05	Si	2.264568175	0.031194512	0.125884	0.2850729	0.00889271	0.09151941
		B		0.058042764	0.069951	0.158408808	0.00919449	
		Na		0.035797516	0.148753	0.33686131	0.0120588	
		AL		0.032310646	0.174583	0.395355106	0.01277418	
		O		0.044359931	0.465851	1.054951349	0.04679757	
	0.2	C	0.053117135	0.014978	0.033918702	0.00180166	0.09498848	
		Si	0.031194512	0.216605	0.514440468	0.01604772		
		B	0.058042764	0.058906	0.139902727	0.00812034		
		Na	0.035797516	0.125266	0.297508828	0.01065008		
		AL	0.032310646	0.147016	0.349165439	0.01128176		
	0.35	O	0.044359931	0.392296	0.931709508	0.04133057	0.09881328	
		C	0.053117135	0.059911	0.142289619	0.00755802		
		Si	0.031194512	0.307325	0.767326316	0.02393637		
		B	0.058042764	0.047861	0.119498917	0.00693605		
		Na	0.035797516	0.101778	0.254118402	0.00909681		
0.5	AL	0.032310646	0.119451	0.29824419	0.00963646	0.10305152		
	O	0.044359931	0.318742	0.795832179	0.03530306			
	C	0.053117135	0.104843	0.261771066	0.01390453			
	Si	0.031194512	0.398046	1.04754878	0.03267777			
	B	0.058042764	0.036817	0.096892328	0.0056239			

**Table 5. Effective removal cross-section for group G+ TiB2**

Group	Concentration	Element	Composite Density(g/cm <sup>3</sup> )	Σ/ρ (cm <sup>2</sup> /g)	Fraction by Weight	Partial Density (g/cm <sup>3</sup> )	Σ(cm <sup>-1</sup> )	TotalΣ(cm <sup>-1</sup> )
G2	0.05	Si	2.287958234	0.031194512	0.090862	0.207888461	0.00648498	0.09201259
		B		0.058042764	0.085506	0.195634157	0.01135515	
		Na		0.035797516	0.148753	0.340340651	0.01218335	
		AL		0.032310646	0.174581	0.399434036	0.01290597	
		O		0.044359931	0.465853	1.065852207	0.04728113	

		Ti		0.022865615	0.034445	0.078808721	0.00180201	
		Si		0.031194512	0.076515	0.189867207	0.00592281	
		B		0.058042764	0.121126	0.300566625	0.01744572	
0.2	2.481437715	Na		0.035797516	0.125266	0.310839777	0.01112729	0.09728328
		AL		0.032310646	0.147016	0.364811047	0.01178728	
		O		0.044359931	0.392296	0.97345809	0.04318253	
		Ti		0.022865615	0.137781	0.34189497	0.00781764	
		Si		0.031194512	0.062169	0.168519202	0.00525687	
		B		0.058042764	0.156746	0.424885567	0.02466153	
0.35	2.710662902	Na		0.035797516	0.101778	0.275885849	0.00987603	0.10352784
		AL		0.032310646	0.119451	0.323791394	0.01046191	
		O		0.044359931	0.318741	0.863999404	0.03832695	
		Ti		0.022865615	0.241115	0.653581486	0.01494454	
		Si		0.031194512	0.047822	0.142822706	0.00445528	
		B		0.058042764	0.192366	0.574510321	0.03334617	
0.5	2.986548148	Na		0.035797516	0.078291	0.233819841	0.00837017	0.11104344
		AL		0.032310646	0.091885	0.274418977	0.00886665	
		O		0.044359931	0.245185	0.732256808	0.03248286	
		Ti		0.022865615	0.344451	1.028719496	0.0235223	

**Table 6. Effective removal cross-section for group G+ BiClO**

Group	Concentration	Element	Composite Density(g/cm <sup>3</sup> )	$\Sigma/\rho$ (cm <sup>2</sup> /g)	Fraction by Weight	Partial Density(g/cm <sup>3</sup> )	$\Sigma$ (cm <sup>-1</sup> )	Total $\Sigma$ (cm <sup>-1</sup> )
G3	0.05	Si	2.312482506	0.031194512	0.090862	0.210116785	0.00655449	0.09071235
		B		0.058042764	0.069951	0.161760464	0.00938902	
		Na		0.035797516	0.148753	0.34398871	0.01231394	
		AL		0.032310646	0.174582	0.403717821	0.01304438	
		O		0.044359931	0.468923	1.084376234	0.04810286	
	0.2	CL	2.601109445	0.02726241	0.006807	0.015741068	0.00042914	0.09168774
		Bi		0.009468693	0.040122	0.092781423	0.00087852	
		Si		0.031194512	0.076515	0.199023889	0.00620845	
		B		0.058042764	0.058906	0.153220953	0.00889337	
		Na		0.035797516	0.125266	0.325830576	0.01166393	
	0.35	AL	2.972059957	0.032310646	0.147016	0.382404706	0.01235574	0.09294114
		O		0.044359931	0.404584	1.052367264	0.04668294	
		CL		0.02726241	0.027226	0.070817806	0.00193066	
		Bi		0.009468693	0.160487	0.417444252	0.00395265	
		Si		0.031194512	0.062169	0.184769995	0.00576381	
0.5	B	3.466413586	0.058042764	0.047861	0.142245762	0.00825634	0.09461178	
	Na		0.035797516	0.101778	0.302490318	0.0108284		
	AL		0.032310646	0.119451	0.355015534	0.01147078		
	O		0.044359931	0.340242	1.011219624	0.04485763		
	CL		0.02726241	0.047646	0.141606769	0.00386054		
	Bi		0.009468693	0.280853	0.834711955	0.00790363		
	Si		0.031194512	0.047822	0.165770831	0.00517114		
	B		0.058042764	0.036817	0.127622949	0.00740759		
	Na		0.035797516	0.078291	0.271388986	0.00971505		
	AL		0.032310646	0.091885	0.318511412	0.01029131		
	O		0.044359931	0.275902	0.956390441	0.04242541		
	CL		0.02726241	0.068065	0.235941441	0.00643233		
	Bi		0.009468693	0.401218	1.390787526	0.01316894		

#### Half-value layer for the neutrons (HVL):

For each combination, Table 7 displays the values of the half-value thickness at various concentrations. As illustrated in Fig 3, a correlation

was established between the additive concentration and the half-value layer. The thickness required to reduce the neutrons' intensity to half its value decreases as reinforcement material increases; this is

because there is a direct correlation between increasing the reinforcing material concentration and the total cross-section<sup>50,51</sup>. Fig 2. Calculated the correlation coefficient by the following equations:  
 $Y_{G1}=0.0251X+0.0902$  .....10  
 $R^2=0.9979$   
 $Y_{G2}=0.0409X+0.0899$  .....11  
 $R^2=0.9936$   
 $Y_{G3}=0.0082X+0.0903$  .....12  
 $R^2=0.9853$   
 X=Concentration of reinforcement material, Y= total cross-section.

**Table 7. The half-value layer for Fast Neutron is at different concentrations of reinforcement material(cm).**

Concentration	G+ SiC	G+TiB <sub>2</sub>	G+ BiClO
0%	7.663080895	7.663080895	7.663080895
5%	7.572176669	7.53159476	7.639539103
20%	7.295630851	7.123530594	7.558271616
35%	7.013243294	6.693859353	7.456332364
50%	6.724791758	6.240804695	7.324669604

Fig 3 establishes a correlation between the reinforcement materials' additive concentration and the half-value layer. The figure shows that the (HVL) required to reduce the neutrons' intensity to half its value decreases as the reinforcement materials' percentage increases due to the correlation between the total cross-section and the percentage increase in reinforcing material concentration. The figure shows the Half-value layer as a function of Concentration for all mixture materials.

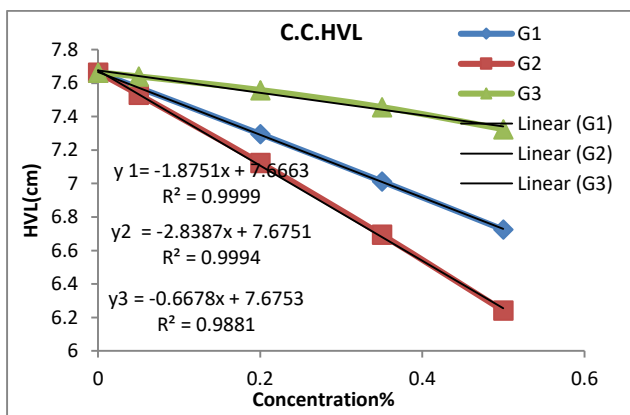


**Figure 3. Half -value layer(cm) as a function of concentration (%) +correlation coefficient**

**The mean free path of the neutrons (MFP):**

The values of the mean free path for different composites and at various concentrations are shown in Table 8.

**Table 8. MFP for Fast Neutron at different Concentrations of reinforcement material.**

Concentration	G+ SiC	G+ TiB <sub>2</sub>	G+ BiClO
0%	11.05783679	11.05783679	11.05783679
5%	10.92666186	10.86810211	11.02386595
20%	10.52760585	10.27926493	10.90659685
35%	10.12012019	9.659248706	10.75949836
50%	9.70388421	9.005490181	10.56950881

The lowest MFP values are seen in the G2 composite, which means it offers the best protection compared to the other mixtures. This may occur due to the homogeneity of the mixture elements; Fig. 4 shows that the mean free path decreases as the concentration of reinforcing materials increases. The shields become denser, and the removal cross-section increases. Therefore, values decrease MFP. This means that increasing density reduces the distance that a particle travels before colliding with another particle, and this may happen as a result of increasing the strength of the mixture and improving its durability, which contributes to a decrease in the free path rate of the neutron within the material. That is consistent with previous studies<sup>14, 52</sup>. calculated the correlation coefficient between the concentrations of the added reinforcing materials and the Mean free path of neutrons for the mixtures being studied. The results indicated a robust and positive correlation, as demonstrated by the following equations:

$Y_{G1}= - 2.7058 X + 11.063$  ..... 13

$R^2=0.9999$

$Y_{G2}= - 4.0962 X + 11.075$  ..... 14

$R^2=0.9994$

$Y_{G3}= - 0.9637 X+ 11.075$  .....15

$R^2=0.9881$

X= Concentration of reinforcement material, Y=mean-free path. Note: A negative sign means that the relationship is inverse between them.

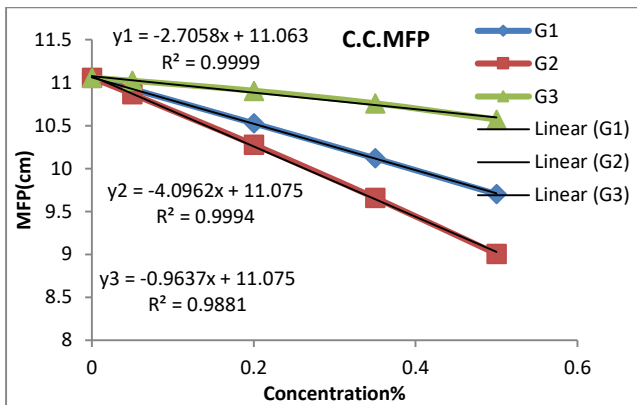


Figure 4. Show the relationship between MFP (cm) and concentration (%) correlation coefficient

## Conclusion

The findings indicated that the macroscopic cross-section of the removal of neutrons depends on the chemical composition of the shielding materials, making it crucial in the selection of materials for fast neutron shielding. The G2 mixture exhibits significant neutron attenuation as a result of the

elevated weight % of boron. Boron is a practical element for absorbing fast neutrons due to its substantial removal cross-section. Adding the reinforcement material ( $\text{TiB}_2$ ) has enhanced the neutron shielding properties of borosilicate glass, making it an efficient barrier against fast neutrons.

## Authors' Declaration

- Conflicts of Interest: None.
- We hereby confirm that all the Figures and Tables in the manuscript are ours. Furthermore, any Figures and images, that are not ours, have been included with the necessary permission for re-publication, which is attached to the manuscript.
- No animal studies are present in the manuscript.
- No human studies are present in the manuscript.
- Ethical Clearance: The project was approved by the local ethical committee at University of Baghdad.

## Authors' Contribution Statement

This work was carried out in collaboration with all authors, S. J. A. and A. F. M., who contributed to the

design and implementation of the results and the writing of the manuscript.

## References

1. Korkut H, Korkut T. Simulations on the performances of neutron shielding glass materials and secondary radiation risks. *Radiation Physics and Chemistry* [Internet]. 2024;223:112020. Available from: <https://doi.org/10.1016/j.radphyschem.2024.112020>
2. Elkhoshkhany N, Marzouk S, El-Sherbiny M, Ibrahim H, Burtan-Gwizdala B, Alqahtani MS, et al. Investigation of structural, physical, and attenuation parameters of glass:  $\text{TeO}_2\text{-Bi}_2\text{O}_3\text{-B}_2\text{O}_3\text{-TiO}_2\text{-RE}_2\text{O}_3$  (RE: La, Ce, Sm, Er, and Yb), and applications thereof. *Materials*. 2022;15(15):5393 <https://doi.org/10.3390/ma15155393>
3. Gaballah M, Issa SAM, Saddeek YB, Elsaman R, Susoy G, Erguzel TT, et al. Mechanical and nuclear radiation shielding properties of different borotellurite glasses: a comprehensive investigation on large  $\text{Bi}_2\text{O}_3$  concentration. *Phys Scr*. 2020;95(8):085701. <https://doi.org/10.1088/1402-4896/ab9bde>
4. Elmahroug Y, Tellili B, Souga C. Determination of

- shielding parameters for different types of resins. *Ann Nucl Energy*. 2014; 63: 619–23. <http://dx.doi.org/10.1016/j.anucene.2013.09.007>
5. Paul MB, Ankan AD, Deb H, Ahasan MM. A Monte Carlo simulation model to determine the effective concrete materials for fast neutron shielding. *Radiat Phys Chem*. 2023; 202: 110476. <https://doi.org/10.1016/j.radphyschem.2022.110476>
  6. Alsaedi JK, Hasan NM, Hassan RG. Properties of Soil in Najaf Governorate. *Ibn AL-Haitham J Pure Appl Sci*. 2018; 31(2): 41–51. <https://jih.uobaghdad.edu.iq/index.php/j/article/view/1942>
  7. Al-Obaidi S, Akyıldırım H, Gunoglu K, Akkurt I. Neutron shielding calculation for barite-boron-water. *Acta Phys Pol A*. 2020;137(4):551–3. <https://doi.org/10.12693/APhysPolA.137.551>
  8. Sariyer D, Küçer R, Küçer N. Neutron shielding properties of concretes containing boron carbide and ferro-boron. *Procedia-Social Behav Sci*. 2015; 195: 1752–6. <https://doi.org/10.1016/j.sbspro.2015.06.320>
  9. Gökmen U. Gamma and neutron shielding properties of B4C particle reinforced Inconel 718 composites. *Nucl Eng Technol*. 2022; 54(3): 1049–61. <https://doi.org/10.1016/j.net.2021.09.028>
  10. Piotrowski T. Neutron shielding evaluation of concretes and mortars: A review. *Constr Build Mater*. 2021; 277: 122238. <https://doi.org/10.1016/j.conbuildmat.2020.122238>
  11. Madbouly AM, El-Sawy AA. Calculation of gamma and neutron parameters for some concrete materials as radiation shields for nuclear facilities. *Int J Emerg Trends Eng Dev*. 2018; 3(8): 7–17. <https://dx.doi.org/10.26808/rs.ed.i8v4.02>
  12. Oto B, Kavaz E, Durak H, Aras A, Madak Z. Effect of addition of molybdenum on photon and fast neutron radiation shielding properties in ceramics. *Ceram Int*. 2019; 45(17, Part B): 23681–9. <https://doi.org/10.1016/j.ceramint.2019.08.082>
  13. El-Khayatt AM, Akkurt İ. Photon interaction, energy absorption and neutron removal cross section of concrete including marble. *Ann Nucl Energy*. 2013; 60: 8–14. <https://doi.org/10.1016/j.anucene.2013.04.021>
  14. Mkhairer AF, Dawood SK. Calculation of Shielding Parameters of Fast Neutrons for Some Composite Materials. *Al-Mustansiriyah J Sci*. 2019; 30(1): 210–5. <https://doi.org/10.21275/ART20177125>
  15. Abd Elwahab NR, Helal N, Mohamed T, Shahin F, Ali FM. New shielding composite paste for mixed fields of fast neutrons and gamma rays. *Mater Chem Phys*. 2019; 233: 249–53. <https://doi.org/10.1016/j.matchemphys.2019.05.059>
  16. Korkut T, Ün A, Demir F, Karabulut A, Budak G, Şahin R, et al. Neutron dose transmission measurements for several new concrete samples including colemanite. *Ann Nucl Energy*. 2010; 37(7): 996–8. <https://doi.org/10.1016/j.anucene.2010.04.005>
  17. Moradillo MK, Chung CW, Keys MH, Choudhary A, Reese SR, Weiss WJ. Use of borosilicate glass powder in cementitious materials: Pozzolan reactivity and neutron shielding properties. *Cem Concr Compos*. 2020; 112: 103640. <https://doi.org/10.1016/j.cemconcomp.2020.103640>
  18. Naseer KA, Marimuthu K, Al-Buriah MS, Alalawi A, Tekin HO. Influence of Bi<sub>2</sub>O<sub>3</sub> concentration on barium-telluro-borate glasses: physical, structural and radiation-shielding properties. *Ceram Int*. 2021; 47(1): 329–40. <https://doi.org/10.1016/j.ceramint.2020.08.138>
  19. Shamshad L, Rooh G, Limkitjaroenporn P, Srisittipokakun N, Chaiphaksa W, Kim HJ, et al. A comparative study of gadolinium based oxide and oxyfluoride glasses as low energy radiation shielding materials. *Prog Nucl Energy*. 2017; 97: 53–9. <https://doi.org/10.1016/j.pnucene.2016.12.014>
  20. Kaur R, Singh S, Pandey OP. FTIR structural investigation of gamma irradiated BaO–Na<sub>2</sub>O–B<sub>2</sub>O<sub>3</sub>–SiO<sub>2</sub> glasses. *Phys B Condens Matter*. 2012; 407(24): 4765–9. <https://doi.org/10.1016/j.ceramint.2020.08.138>
  21. Al-Saadi AJ, Saadon AK. Gamma Ray Attenuation Coefficients for Lead Oxide and Iron Oxide Reinforced In Silicate Glasses as Radiation Shielding Windows. *Ibn AL-Haitham J Pure Appl Sci*. 2017; 27(3): 201–214.
  22. Baykal D Sen, Kilic G, Ilik E, Kavaz E, AlMisned G, Cakirli RB, et al. Designing a Lead-free and high-density glass for radiation facilities: Synthesis, physical, optical, structural, and experimental gamma-ray transmission properties of newly designed barium-borosilicate glass sample. *J Alloys Compd*. 2023; 965: 171392. <https://doi.org/10.1016/j.jallcom.2023.171392>
  23. Zanotto ED, Mauro JC. The glassy state of matter: Its definition and ultimate fate. *J Non Cryst Solids*. 2017; 471: 490–5. <https://doi.org/10.1016/j.jnoncrysol.2017.05.019>
  24. Lee JC, Jang BK, Shon CS, Kim JH, Chung CW. Potential use of borosilicate glass to make neutron shielding mortar: Enhancement of thermal neutron shielding and strength development and mitigation of alkali-silica reaction. *J Clean Prod*. 2019; 210: 638–45. <https://doi.org/10.1016/j.jclepro.2018.11.033>
  25. Singh VP, Badiger NM, Chanthima N, Kaewkhao J. Evaluation of gamma-ray exposure buildup factors and neutron shielding for bismuth borosilicate glasses. *Radiat Phys Chem*. 2014; 98: 14–21. <https://doi.org/10.1016/j.radphyschem.2013.12.029>
  26. Salama E, Maher A, Youssef GM. Gamma radiation and neutron shielding properties of transparent alkali borosilicate glass containing lead. *J Phys Chem Solids*. 2019; 131: 139–47. <https://doi.org/10.1016/j.jpccs.2019.04.002>
  27. Rammah YS, Mahmoud KA, Kavaz E, Kumar A, El-Agawany FI. The role of PbO/Bi<sub>2</sub>O<sub>3</sub> insertion on the

- shielding characteristics of novel borate glasses. *Ceram Int.* 2020; 46(15): 23357–68. <https://doi.org/10.1016/j.ceramint.2020.04.018>
28. Yilmaz AH, Ortaç B, Yilmaz SS. Boron and Boron Compounds in Radiation Shielding Materials. 2023; <https://doi.org/10.5772/intechopen.111858>
29. 29- Saud HA. Gamma ray and neutron shielding properties of bismuth phosphate glass containing iron and barium. *SOP Trans Appl Phys.* 2014; 1(3). <https://doi.org/10.15764/APHY.2014.01001>
30. Elsheikh NAA. Gamma-ray and neutron shielding features for some fast neutron moderators of interest in <sup>252</sup>Cf-based boron neutron capture therapy. *Appl Radiat Isot.* 2020; 156: 109012. <https://doi.org/10.1016/j.apradiso.2019.109012>
31. Abdulrahman ST, Thomas S, Ahmad Z. *Micro and Nanostructured Composite Materials for Neutron Shielding Applications.* Woodhead Publishing; 2020. <https://doi.org/10.1016/C2019-0-00001-5>
32. Bagheri R, Khorrami Moghaddam A, Yousefnia H. Gamma Ray Shielding Study of Barium–Bismuth–Borosilicate Glasses as Transparent Shielding Materials using MCNP-4C Code, XCOM Program, and Available Experimental Data. *Nucl Eng Technol.* 2017; 49(1): 216–23. <https://doi.org/10.1016/j.net.2016.08.013>
33. El Abd A, Mesbah G, Mohammed NMA, Ellithi A. A simple method for determining the effective removal cross section for fast neutrons. *J Radiat Nucl Appl.* 2017; 2(2): 53–8. <http://dx.doi.org/10.18576/jrma/02020>
34. Gaylany, Bozkurt A , Barış A. Investigating thermal and fast neutron shielding properties of B<sub>4</sub>C, B<sub>2</sub>O<sub>3</sub>, Sm<sub>2</sub>O<sub>3</sub>, and Gd<sub>2</sub>O<sub>3</sub> doped polymer matrix composites using Monte Carlo simulations. *Süleyman Demirel Univ Fac Arts Sci J Sci.* 2021; 16(2): 490–9. <https://doi.org/10.29233/sdufeffd.933338>
35. Mkhaimer A, Al-Bayati A, Fadhil I. Investigation of fast neutron attenuation coefficients for some Iraqi building materials. *Malaysian J Sci.* 2022; 80–9. <https://doi.org/10.22452/mjs.vol41no2.7>
36. Gaballah M, Issa SAM, Saddeek YB, Elsaman R, Susoy G, Erguzel TT, et al. Mechanical and nuclear radiation shielding properties of different borotellurite glasses: a comprehensive investigation on large Bi<sub>2</sub>O<sub>3</sub> concentration. *Phys Scr.* 2020;95(8):85701. <https://doi.org/10.1088/1402-4896/ab9bde>
37. Ghasemi-Jangjoo A, Ghiasi H. MC safe bunker designing for an 18MV linac with nanoparticles included primary barriers and effect of the nanoparticles on the shielding aspects. *Reports Pract Oncol Radiother.* 2019; 24(4): 363–8. <https://doi.org/10.1016/j.rpor.2019.05.009>
38. Sttar MAK, Mkhaimer AF, Majeed AMA. Study of the effect of using nanomaterial in radiological shielding. *AIP Conf Proc.* 2019; 2190(1): 1-7. <https://doi.org/10.1063/1.5138563>
39. Mkhaimer AF, Majeed AMA. The effect of using Nano iron oxide in radiological shielding. *IOP Conf Ser Mater Sci Eng* 2020. 928: 72033. <https://doi.org/10.1088/1757-899X/928/7/072033>
40. Clyne TW, Hull D. *An introduction to composite materials.* Cambridge university press; 2019.p.37
41. Anand R, Manickam C, Naveen G. Investigation Of Polycarbonate Plastic With Composite Material. *Int J Sci Adv Res. Technol.* 2018 ;4(3): 2451-2456.
42. Siraj S, Al-Marzouqi AH, Iqbal MZ, Ahmed W. Impact of micro silica filler particle size on mechanical properties of polymeric based composite material. *Polymers (Basel).* 2022; 14(22): 4830. <https://doi.org/10.3390/polym14224830>
43. El-Khayatt AM. Calculation of fast neutron removal cross-sections for some compounds and materials. *Ann Nucl Energy.* 2010; 37(2): 218–22. <https://doi.org/10.1016/j.anucene.2009.10.022>
44. Uddin Z, Yasin T, Shafiq M, Raza A, Zahur A. On the physical, chemical, and neutron shielding properties of polyethylene/boron carbide composites. *Radiat Phys Chem.* 2020; 166: 108450. <https://doi.org/10.1016/j.radphyschem.2019.108450>
45. Dong MG, Xue XX, Elmahroug Y, Sayyed MI, Zaid MHM. Investigation of shielding parameters of some boron containing resources for gamma ray and fast neutron. *Results Phys.* 2019;13:102129. <https://doi.org/10.1016/j.rinp.2019.02.065>
46. Tekin HO, Altunsoy EE, Kavaz E, Sayyed MI, Agar O, Kamislioglu M. Photon and neutron shielding performance of boron phosphate glasses for diagnostic radiology facilities. *Results Phys.* 2019; 12: 1457–64. <https://doi.org/10.1016/j.rinp.2019.01.060>
47. Evans BR, Lian J, Ji W. Evaluation of shielding performance for newly developed composite materials. *Ann Nucl Energy.* 2018; 116: 1–9. <https://doi.org/10.1016/j.anucene.2018.01.022>
48. Sayyed MI. Investigations of gamma ray and fast neutron shielding properties of tellurite glasses with different oxide compositions. *Can J Phys.* 2016; 94(11): 1133–7. <https://doi.org/10.1139/cjp-2016-0330>
49. Rawi KRA Al. Design and Testing a Neutrons and Gamma-Rays Multilayer Shield Using Different Groups of Cross-Sections. *Baghdad Sci J.* 2010; 7(3): 1120–1126. <https://doi.org/10.21123/bsj.2010.7.3.1120-1126>
50. Afkham Y, Mesbahi A, Alemi A, Zolfagharpour F, Jabbari N. Design and fabrication of a Nano-based neutron shield for fast neutrons from medical linear accelerators in radiation therapy. *Radiat Oncol.* 2020; 15(1): 1–13. <http://dx.doi.org/10.1186/s13014-020-01551-1>
51. Shafik SS, Rejah BK, Mahmood RR, Fazaa WT. Study the Shielding Properties against Gamma-rays for Epoxy Resin Reinforced by Different materials. *Baghdad Sci J.* 2016; 8(3): 705–710.

<https://doi.org/10.21123/bsj.2011.8.3.705-710>

52. Mkhahber AF, Al-Bayati AT, Hussein IF. Investigation of fast neutron attenuation coefficients for some Iraqi

building materials. Malaysian J Sci. 2022;41(2):81–9.

<https://doi.org/10.22452/mjs.vol41no2.7>

## دراسة تأثير بعض المواد المضافة لزجاج البوروسليكات على خصائص التدرج النيوتروني

صدام جميل عبد نور، أحمد فاضل مخيبر

قسم الفيزياء، كلية التربية أبن-الهيثم، جامعة بغداد، بغداد، العراق

### الخلاصة

يعد تطوير مواد الحماية من الإشعاع أمراً مهماً نظراً لاستخدام المصادر المشعة في الصناعة والطب والزراعة. ونتيجة لذلك، تم إجراء المزيد من البحث والتطوير للنظر في أنظمة زجاجية مختلفة بناءً على صفاتها الفريدة للحماية من الإشعاع النيوتروني. تركز هذه الدراسة على دراسة المواد ذات الأساس الزجاجي لأغراض الحماية النيوترونية. يتعمق هذا البحث في خصائص التدرج النيوتروني لخليط يشتمل على زجاج بوروسليكات المنيوم الصوديوم  $(\text{SiB}_2\text{Na}_2\text{Al}_2\text{O}_9)_x$ ، مع إضافة مواد تدعيم  $(\text{SiC})_{100-x}$ ،  $(\text{TiB}_2)_{100-x}$  و  $(\text{BiClO})_{100-x}$  حيث،  $(X=95, 80, 65, \text{ and } 50\%)$  ويشار إلى المخاليط بالرمز G1 و G2 و G3 على التوالي. تشير النتائج والحسابات إلى أن إضافة مواد التدعيم إلى زجاج البوروسليكات بكميات مختلفة يعزز الإزالة السريعة للنيوترونات ( $\Sigma_R$ ). تعمل زيادة نسبة التعزيز على تقليل قيمة سمك النصف للدرع (HVL) ومتوسط المسار الحر (MFB) للنيوترون. بمقارنة النتائج النظرية، فإن إضافة نتريد التيتانيوم ( $\text{TiB}_2$ ) كمادة تعزيز إلى زجاج البوروسليكات يؤدي إلى الحد الأقصى من التوهين النيوتروني وأقل قيمة HVL عند  $X = 50$ . وبالتالي فإن درع G2 هو الأفضل للحماية من الإشعاع النيوتروني.

**الكلمات المفتاحية:** نيوترون سريع، قيمة سمك النصف، متوسط المسار الحر، المقطع العرضي للإزالة، مادة التدرج.